Chemical Engineering Science
May 2010 ; Volume 65 (10) : Pages 3313-3321
http://dx.doi.org/10.1016/j.ces.2010.02.019

Dynamical modelling of a reactive extrusion process: Focus on residence time distribution in a fully intermeshing co-rotating twin-screw extruder and application to an alginate extraction process

Régis Baron[a, *], Peggy Vauchel[b,c, *], Raymond Kaas[a], Abdellah Arhaliass[d], Jack Legrand[d]

[1] IFREMER, Dpt. BRM, rue de l'Ile d'Yeu, BP 21105, 44311 Nantes Cedex 03, France
[2] Univ Lille Nord de France, F-59000 Lille, France
[3] USTL, Laboratoire ProBioGEM, F-59650 Villeneuve d'Ascq, France
[4] GEPEA, Université de Nantes, CNRS, UMR6144, 37 bd de l'Université, BP 406, 44602 Saint-Nazaire Cedex, France

*: Corresponding author : Régis Baron, email address : rbaron@ifremer.fr, Peggy Vauchel, email address : peggy.vauchel@polytech-lille.fr

Abstract:

The context of this study is the modelling of reactive extrusion process based on an alginate extraction protocol. Residence Time Distribution (RTD) is one important part to predict the kinetics of reactive compounds. A simple model is proposed to predict RTD in fully intermeshing co-rotating twin-screw extruders without reaction. This model, which can be easily extended to reactive case in a future work, is based on the extension of an axial dispersion model, including control parameters (screw speed and flow rate) and geometrical parameters (screw profile and die design). Simulations were performed for various operating and geometrical conditions so as to illustrate possibilities offered by the proposed model. Validation was conducted for two different extrusion applications, seaweed extrusion and polymer extrusion. This highlighted the model ability to predict RID for various kinds of materials after adjusting only one parameter thanks to a unique experimental RID curve.

Keywords: Alginate, Extraction, Extrusion, Mathematical modeling, Residence time distribution, Simulation, *Laminaria digitata*

Notation

a, b, c and *d* : piecewise constant functions depending on screw geometry (m6, m3, m3 and m6 respectively) (Equation 10)
C : tracer concentration (mol.m-3 or g.m-3),
Cin : input tracer concentration (mol.m-3 or g.m-3)
D: screw diameter (m)
Dax : axial dispersion function (m².s-1)
Fdi and *Fpi* : parameters depending on the channel narrowness in screw zone *i* (Equation 8)
Hi : channel height of screw zone *i* (m)
i : screw zone index (Figure 2)
j : spatial discretization index associated to the last fully filled zone (Figure 2)

K : parameter depending on the die geometry (m^3) (Equation 9)

l : length of fully filled channel (m) (Equation 12)

l_i : channel length of screw zone i (m)

l_{tot} : total length of the screw channel (partially + fully filled) (m) (Figure 2)

LDPE : low density polyethylene

m : number of elements for spatial discretization

n : number of fully filled screw zones (Figure 2)

n_{tot} : total number of screw zones (Figure 2)

N : screw speed ($rad.s^{-1}$)

P : pressure (Pa)

P_d : pressure at the head of the die (Pa)

Q : input flow rate ($m^3.s^{-1}$)

Q_{ci} : flow rate in the channel of screw zone i ($m^3.s^{-1}$)

Q_{out} : output flow rate ($m^3.s^{-1}$)

r : algae feed rate to reactive solution feed rate ratio

RTD : residence time distribution

S_i : section of the channel in screw zone i (m^2)

t : time (s)

v : fluid speed ($m.s^{-1}$)

v_{bx}, v_{bz} : boundary values of fluid speed ($m.s^{-1}$) (Equations 3 and 5)

V_b : barrel speed ($m.s^{-1}$) (Figure 1)

V_i : volume of the channel in screw zone i (m^3)

W_i : width of the channel in screw zone i (m)

z : abscissa along the unrolled screw channel

α_i and β_i : parameters depending on the geometry of screw zone *i* (m^3 and m^6 respectively) (Equation 8)

λ_1 *and* λ_2 : correction parameter relative to axial dispersion function D_{ax} in the fully filled zone and in the partially filled zone respectively (Equation 16)

μ : fluid viscosity (Pa.s)

θ_i : pitch angle in screw zone *i* (rad)

1. INTRODUCTION

Extrusion is a continuous process consisting in shaping or in transforming a material within a screw/barrel system. Mostly, the involved mechanisms are purely thermo-mechanical. Reactive extrusion process, which consists in using extruders as chemical reactors, has developed since few decades. For some applications, it appears as an interesting alternative to batch process, with several advantages due to the fact that it is a continuous process, its modularity (screw profile can be adapted to each application and several zones can be created along the screw to conduct different steps), its thermal regulation facilitated by a favourable surface/volume ratio and its ability to work with high viscosity products, enabling solvent consumption limitation (gains in waste treatment and process safety) (Berzin and Hu, 2004). Most of developed reactive extrusion applications deal with polymer science or food fields. Several applications have also been developed with biological raw materials, mostly for biomolecules extraction or for by-products upgrading (Perrin and De Choudens, 1996; N'Diaye et al., 1996; Dufaure et al., 1999; Rouilly et al., 2006). Hence, a previous work highlighted the interest of reactive extrusion process when extracting alginate from brown algae in terms of extraction yield, time, reactant and water demand and alginate rheological properties (Vauchel et al., 2008a).

Reactive extrusion modelling is essential to help understanding phenomena taking place in the extruder, optimization and scale up. The model structure adopted for alginate extraction application is based on the combination of an extraction kinetics model and one describing material flow inside the extruder. The extraction kinetics model was presented in a previous paper (Vauchel et al., 2008b). The current paper aims at modelling the material flow inside the extruder based on residence time distribution. The coupling between both models will be discussed in a forthcoming paper. Residence time distribution (RTD) is a particularly important parameter in reactive extrusion process as it is directly linked to contact time of reactants. Few authors have proposed models for reactive extrusion processes based on the coupling of a RTD model and kinetics model for chemical reaction and/or for viscosity (Ganzeveld and Janssen, 1993; Prat et al., 1999, 2002; Puaux et al., 2006). RTD models are generally built by fitting experimental RTD curves with different flow models (Ainser, 1996; Puaux et al., 2000). Good correlations have been obtained, especially with the backflow cell model and the axial dispersion model. Nevertheless these models don't directly take into account the geometrical parameters (screws profile and die design) and the control parameters (screw speed and flow rate). These points limit the prediction value of this modelling approach especially when scaling up.

The present paper aims at presenting a model enabling to predict the residence time distribution in fully intermeshing twin-screw extrusion process and including all geometrical and control parameters. At first, the physical considerations and hypotheses taken into account are described. Simulations of residence time distribution, in various conditions, are then presented and discussed. The model is then validated in the case of seaweeds and polymer extrusion.

2. RESIDENCE TIME DISTRIBUTION MODEL

2.1. Seaweeds extrusion process considerations

In seaweeds extrusion application, material flowing in the extruder evolves along the screw channels. In the feeding section, two different phases are injected, a solid one composed of seaweeds cut in pieces, and a liquid one composed of a sodium carbonate solution. However, reaction between seaweeds and reactive solution takes place very rapidly in the extruder (under the combined effects of a sodium carbonate chemical action and the shearing provided by the screws) resulting shortly in a pseudo-homogenous phase. Experiments of instantaneous stop and opening of the extruder showed that it appears in the first third of the screw channels in all cases. This pseudo-homogenous phase is composed of a viscous sodium alginate solution with very small (less than 1mm diameter) seaweed particles in suspension. The goal of this work is to build a simple model for RTD prediction. To assure the assumption of a homogenous fluid flowing all along the screw channels, seaweeds under the form of a pseudo homogeneous phase were run twice through the extruder. Tracer experiments for validation, which is presented in a further section, were carried out during the second extrusion run.

2.2. RTD model description

The spatiotemporal tracer concentration evolution is described by means of an axial dispersion model with two parameters depending on the length of the fully filled channel, the axial dispersion coefficient and fluid speed. The final proposed RTD model is based on the combination of a tracer concentration evolution model and a model for the calculation of the length of a fully filled channel, which are both described below.

2.2.1. Length of fully filled channel model

The adopted approach to determine the length(s) of fully filled channel is based on elements described by Baron (1995). A simplified solution of the Navier-Stokes equations is used to describe fluid flow at steady state in a fully intermeshing co-rotating twin-screw extruder. To solve the Navier-Stokes equations, several simplifying assumptions have to be considered concerning extruder geometry, fluid properties and flow type.

It is assumed that the screw channel is unrolled and fixed, and that the barrel is plane and slides on the screw channel at V_b velocity (Figure 1). The totally unrolled channel length l_{tot} is divided into n_{tot} zones, corresponding to different screw element geometries composing the screw profile. The correspondence between the abscissa z along the unrolled screw channel and the iteration i for screw zones of different geometries is described in Figure 2. Filling of the screw channel occurs in the opposite direction to the flow (behind the die or reverse pitch screw elements). Hence, it was simpler to perform calculation iteration from the die to the feeding section (see axes directions for i, j and z on Figure 2). The fluid is assumed to be incompressible, Newtonian, and viscosity is assumed to be constant along the screws. The flow is assumed to be established, laminar, isothermal and uniform along the screw channel, which length is considered as infinite (width to length of the channel ratio as well as height to length of the channel ratio are assumed to be close to zero). If the interpenetration zone of the screws is neglected it can be assumed that the channel passes from one screw to the other without leakage or flow restriction. Gravity forces can be neglected compared to others forces as well as inertial forces compared to viscous forces.

$$\begin{cases} \dfrac{\partial P}{\partial x} = \mu \cdot \dfrac{\partial^2 v_x(y)}{\partial y^2} \\ \dfrac{\partial P}{\partial y} = 0 \\ \dfrac{\partial P}{\partial z} = \mu \cdot \left(\dfrac{\partial^2 v_z(x,y)}{\partial x^2} + \dfrac{\partial^2 v_z(x,y)}{\partial y^2} \right) \end{cases} \tag{1}$$

(2) $$v_x(y=0)=0$$

(3) $$v_x(y=H)=-v_{bx}=-\pi \cdot D \cdot N \cdot \sin\theta$$

(4) $$v_z(x,y=0)=0$$

(5) $$v_z(x=0,y=H)=v_{bz}=\pi \cdot D \cdot N \cdot \cos\theta$$

(6) $$v_z(x=0,y)=0$$

By doing so, a linear form of the Navier-Stokes equations can be obtained, which can be simplified according to Equation system 1. If the boundary conditions described by Equations 2 to 6 are taken into account, Equation system 1 can be solved to get fluid speed components expressions according to the solution described by Tadmor and Klein (1970).

(7) $$Q_c=\int_0^H\int_0^W v_z \cdot dy \cdot dx$$

(8) $$Q_{ci}=\alpha_i \cdot N-\frac{\beta_i}{\mu \cdot S_i}\cdot\frac{\partial P}{\partial z} \text{ with } \alpha_i=\frac{\pi \cdot D \cdot \cos\theta_i \cdot W_i \cdot H_i \cdot F_{di}}{2} \text{ and}$$

$$\beta_i=\frac{(W_i \cdot H_i^2)^2 \cdot F_{pi}}{12}$$

The flow rate in the screw channel at abscissa z (Q_c) is then obtained by solving Equation 7. Its expression (Equation 8) is assumed to be the difference between a pumping flow rate depending on the screw speed N and a drag flow rate depending on the pressure gradient $\frac{\partial P}{\partial z}$ (Janssen et al., 1979; Tadmor and Klein, 1970). It holds true for each type of screw element, direct or reverse screw pitch for example. Screw geometry is taken into account via parameters α and β (with correction factors F_{di} and F_{pi} to take into account the impact of a limit layer in the screw channel).

(9) $$Q_{out}=\frac{K}{\mu}\cdot P_d$$

(10) $$Q_{out} = \left(\frac{a + b \cdot l \cdot S}{c + \frac{d}{K} + l \cdot S} \right) \cdot N \text{, with } a = \sum_{i=1}^{n-1} \left(\alpha_i \cdot \frac{\beta_n}{\beta_i} - \alpha_n \right) \cdot V_i \text{ , } b = \alpha_n \text{ ,}$$

$$c = \sum_{i=1}^{n-1} \left(\frac{\beta_n}{\beta_i} - 1 \right) \cdot V_i \text{ and } d = \beta_n \text{ , for } \sum_{i=0}^{n+1} \frac{V_i}{S_i} < l < \sum_{i=0}^{n} \frac{V_i}{S_i} .$$

As the outflow rate Q_{out} is constrained by the die, it is assumed to follow a Hagen-Poiseuille equation (Equation 9). It depends on the pressure at the end of the die (P_d), which is equal to atmospheric pressure and on the geometrical coefficient K, which is inversely proportional to the flow restriction. Moreover, the output pressure of the iteration zone 1 is assumed to be equal to the pressure present at the head of the die, and the output pressure of iteration zone i to be equal to the input pressure of the iteration zone i-1. Consequently, pressure gradients can be eliminated in the flow rate expression (Equation 8) resulting in the outflow rate expression presented in Equation 10 (Baron, 1995). a, b, c and d are piecewise constant functions, depending on screw geometry.

(11) $$\frac{dl}{dt} = \frac{Q(t-\tau) - Q_{out}}{S_n}$$

(12) $$l = \frac{-a + \left(c + \frac{d}{K} \right) \cdot \frac{Q}{N}}{\left(b - \frac{Q}{N} \right) . S_n}$$

Hence, length of the fully filled channel l can be obtained by solving a dynamical equation traducing mass balance (Equation 11). τ is a pure delay depending on control parameters and length of starved screw (l_{tot}-l) and describing the conveying time in the feeding zone. Carrot et al. (1993) proposed a specific flow model for this area. At steady-state, the outflow rate Q_{out} is equal to the input flow rate Q, and the fully filled channel length l can be estimated by Equation 12.

In the case of a screw profile containing restrictive elements (reverse screw pitch or kneading discs for example), several fully filled channel zones appear along the screws. The proposed model enables to deal with these cases. Two examples are given below, one in the case of a unique fully filled channel zone, the second one in the case of several fully filled channel zones. Screw profiles, corresponding to validation experiments with seaweeds exposed in a further section, are described in Figure 3.

Example 1 (Profile 1)

Screw profile is described in Figure 3a. Each zone corresponds to a different type of screw element and is characterized by four functions depending on its geometry, l_i, S_i, α_i and β_i. In this case, there is only one fully filled zone. Matter fills the screw channel from the die to the feeding zone.

If $l<(l_3+l_2+l_1)$ (Figure 3b), then $a=(\alpha_1\cdot\frac{\beta_3}{\beta_1}-\alpha_3)\cdot S_1\cdot l_1+(\alpha_2\cdot\frac{\beta_3}{\beta_2}-\alpha_3)\cdot S_2\cdot l_2$

$b=\alpha_3$

$c=(\frac{\beta_3}{\beta_1}-1)\cdot S_1\cdot l_1+(\frac{\beta_3}{\beta_2}-1)\cdot S_2\cdot l_2$

$d=\beta_3$.

If $(l_3+l_2+l_1)\leq l<(l_4+l_3+l_2+l_1)$ (Figure 3c), then

$a=(\alpha_1\cdot\frac{\beta_4}{\beta_1}-\alpha_4)\cdot S_1\cdot l_1+(\alpha_2\cdot\frac{\beta_4}{\beta_2}-\alpha_4)\cdot S_2\cdot l_2+(\alpha_2\cdot\frac{\beta_4}{\beta_2}-\alpha_4)\cdot S_3\cdot l_3$

$b=\alpha_4$

$c=(\frac{\beta_4}{\beta_1}-1)\cdot S_1\cdot l_1+(\frac{\beta_4}{\beta_2}-1)\cdot S_2\cdot l_2+(\frac{\beta_4}{\beta_2}-1)\cdot S_3\cdot l_3$

$d=\beta_4$.

And so on …

For reverse pitch or kneading disc elements, we assumed that they act like a direct pitch element. α, β and a mean adjusted section S can be assessed by specific experiments not discussed here.

Example 2 (Profile 2)

In this case, screw profile contains two restrictive elements zones (Figure 3d), which implies two fully filled zones (l_2^*, l_3^*) on top of the one implied by the die (l_1*). These lengths are characterized by equations similar to equation (13) . For l_2^* and l_1^*, the input flow corresponds to the output flow of the previous fully filled zone but with a specific pure delay. For each fully filled zone l_i*, functions a_i*,b_i*, c_i* and d_i* are defined, just as described above.

For example (Figure 3e), if $l_1^* < (l_3 + l_2 + l_1)$ then,

$$a_1^* = (\alpha_1 \cdot \frac{\beta_3}{\beta_1} - \alpha_3) \cdot S_1 \cdot l_1 + (\alpha_2 \cdot \frac{\beta_3}{\beta_2} - \alpha_3) \cdot S_2 \cdot l_2$$

$$b_1^* = \alpha_3$$

$$c_1^* = (\frac{\beta_3}{\beta_1} - 1) \cdot S_1 \cdot l_1 + (\frac{\beta_3}{\beta_2} - 1) \cdot S_2 \cdot l_2$$

$$d_1^* = \beta_3;$$

If $l_2^* < (l_6 + l_5 + l_4)$ then,

$$a_2^* = (\alpha_4 \cdot \frac{\beta_6}{\beta_4} - \alpha_6) \cdot S_4 \cdot l_4 + (\alpha_5 \cdot \frac{\beta_6}{\beta_5} - \alpha_6) \cdot S_5 \cdot l_5$$

$$b_2^* = \alpha_6$$

$$c_2^* = (\frac{\beta_6}{\beta_4} - 1) \cdot S_4 \cdot l_4 + (\frac{\beta_6}{\beta_5} - 1) \cdot S_5 \cdot l_5$$

$$d_2^* = \beta_5$$

If $l_3^* < (l_9 + l_8 + l_7)$ then,

$$a_3^* = (\alpha_7 \cdot \frac{\beta_9}{\beta_7} - \alpha_9) \cdot S_7 \cdot l_7 + (\alpha_8 \cdot \frac{\beta_9}{\beta_8} - \alpha_9) \cdot S_8 \cdot l_8$$

$$b_3^* = \alpha_9$$

$$c_3^* = (\frac{\beta_9}{\beta_7} - 1) \cdot S_7 \cdot l_7 + (\frac{\beta_9}{\beta_8} - 1) \cdot S_8 \cdot l_8$$

$$d_3^* = \beta_9$$

It is easy to generalize Equations 10 and 11 to the case of overlapping fully filled zones.

2.2.2. Model for tracer concentration

A largely used approach is based on the description of the flow pattern by conceptual models, combining ideal reactors, which represent the overall features of the physical flow. But residence time distributions commonly encountered in twin-screw extrusion present intermediate characteristics between those obtained with two ideal limiting cases, the perfect mixer and the plug flow reactor. Therefore, non-ideal models have to be used to describe the material flow. One of the main significant criteria for an extrusion flow model is its ability to describe with sufficient flexibility the axial mixing along the screw. Two models seem to better fulfil this requirement, the one-parameter axial dispersion model and the two-parameter backflow cell model (Puaux et al., 2000).

In this paper, the axial dispersion model has been chosen. It consists in a combination of the convective transport and an eddy diffusion mechanism in the axial direction.

(13) $$\frac{\partial C}{\partial t} = D_{ax} \cdot \frac{\partial^2 C}{\partial z^2} - v \cdot \frac{\partial C}{\partial z}$$

For a constant fluid velocity v and a constant axial dispersion coefficient D_{ax} along the flow axis z, the spatio temporal tracer concentration evolution can be described by Equation 13.

(14) $v(z) = \psi \cdot N$ for $l < z \leq l_{tot}$

(15) $$v(z)=\frac{Q}{S(z)} \text{ for } 0<z\le l$$

(16) $$D_{ax}(z)=\lambda(z)\cdot\left|\alpha(z)\cdot N-Q\right|$$

with $\lambda(z)=\lambda_1$ for $0 < z \le l$ and $\lambda(z)=\lambda_2$ for $l < z \le l_{tot}$

Equation 13 has been extended to the case where D_{ax} and v functions are piecewise constant. The fluid velocity v depends on the fully filled length l: when the screw channel is partially filled ($l<z<l_{tot}$), it depends on the pumping effect (Equation 14) whilst when the channel is fully filled ($0\le z\le l$), it depends on the global outflow rate (Equation 15). Equation (14) is an approximate law for the starved screw. The value of ψ can be assessed by literature (Carrot et al., 1993) or experimentally fitted. In the conveying area, the throughput is the result of a transport phenomenon in the intermeshing zone and then, when this zone is fully filled, of a pumping flow in the C-channel area. In the intermeshing zone, material moves forward in the axial direction a distance equivalent to the pitch for every screw revolution, whatever the operating conditions are. In the channels, material conveying is mainly due to the friction of solid polymer with both barrel and screw. Equation (15) expresses the mean velocity of matter in the fully filled zone. According to Equation 16, the axial dispersion coefficient D_{ax} depends on the flow regime. The term αN-Q takes into account the pressure gradient influence on dispersion and the λ correction parameter is thought to modulate the value of the axial dispersion function D_{ax} by taking into account the screw channel filling.

(17) $$D_{ax}\frac{\partial C}{\partial z}=v\cdot(C-C_{in}) \text{ for } z=l_{tot}$$

(18) $$\frac{\partial C}{\partial z}=0 \text{ for } z=0$$

Tracer output concentration was estimated by numerical solving of Equation 13, boundary conditions being defined by Equation 17 and 18 (finite difference approximation has been used for partial derivatives).

3. SIMULATIONS

In order to illustrate the possibilities offered by the proposed model several simulations are presented in this part. It enables to simulate RTD in function of process parameters (flow rate and screw speed) and geometrical parameters (screw profile and die design). Simulations were performed with Matlab software (Simulink toolbox). A 100 units pulse of tracer from t=0 to t=2s at the feeding section of the extruder was considered. All simulations presented in this paper were performed with m=100 spatial discretization elements.

Figure 4 illustrates the RTD evolution in function of process and geometrical parameters within the frame of the explored experimental domain. Increasing screw speed leads to a decrease of RTD pure delay and dispersion. An increasing flow rate leads also to a distribution width decrease and to a more Gaussian distribution shape (Figure 4a&b). By increasing the screw pitch mean residence time increases and distribution become larger. For a low screw speed, pure time-delay (delay before tracer concentration increase) increases with screw pitch, whereas for a high screw speed, pure time-delay is not influenced by screw pitch. Increasing restriction at the die leads to a larger distribution, but has no influence on pure time-delay (Figure 4c&d). Observed tendencies are in agreement with what is commonly described in literature. These above calculations show that the influence of process and geometrical parameters can be simulated thanks to the proposed model, which could be useful for die and screw profile design.

4. VALIDATION

In order to work in absolutely homogeneous conditions, experiments with *Laminaria digitata* were, as explained before, carried out during a second run through the extruder. Hence, alkaline reaction had already occurred and only mechanical properties where involved in material flow.

Model validation was performed in the case of a constant viscosity along the screws with experimental data from two different extrusion applications, reactive extrusion of seaweeds for alginate extraction and LDPE (low density polyethylene) extrusion. Seaweed extrusion experiments are described below and polymer extrusion data were obtained from Puaux et al. (2000). Assumption of a constant viscosity is maintained for polymer experiments even if authors are perfectly aware that this assumption appears extremely limitative.

4.1. Seaweeds extrusion

4.1.1. Experimental

Validation for the proposed RTD model was performed with experimental data obtained from a seaweed reactive extrusion application developed by Vauchel et al. (2008). A carbonatation step by means of reactive extrusion is applied to extract alginate from brown seaweeds. The alginate extraction protocol was adapted from the industrial process described by Pérez et al. (1992).

All experiments were conducted on two-year-old *Laminaria digitata* fronds harvested in Portsall, Brittany, France. The entire fronds were cut into small pieces ($5mm^2$ - $5cm^2$) by means of a separator (RM70S type provided by LIMA S.A.S., Quimper, France) and stored in a 2% (w/w) formalin solution to ensure their preservation during stocking (about 4 months). Before each extraction experiment, algae pieces were rinsed with distilled water in order to eliminate any formalin present, immersed in a 0.5M H_2SO_4 solution for at least one night (stored at 4°C), and rinsed again with distilled water to eliminate excess acid. The alkaline extraction step was conducted in a corotative twin-screw extruder (BC21 type provided by Clextral, Firminy, France) equipped with a 4mm diameter and 5cm long cylindrical die. Algae pieces were introduced in the hopper and the feed rate was regulated by means of a feed pump. An external volumetric pump was used to supply the extruder with a 5% (w/w) Na_2CO_3 solution. As alginate starts to degrade at 40°C, the barrel temperature was maintained at about 20°C thanks to a circulating cooling water system.

Two different screw profiles were used, a simple one composed of decreasing direct pitch screw elements and a small reverse screw element (profile 1 in Figure 3a) and a restrictive one including two kneading discs sections (profile 2 in Figure 3d). As Algae feed rate to reactive solution feed rate ratio (r) influences process efficiency, two different values for this parameter were also considered, r=1 and r=3. They correspond to the boundary values of r for the experimental area where seaweeds extrusion operates. All experiments were undertaken for a fixed screw speed and a global feed rate of respectively 300rpm and 4kg.h^{-1}.

Experimental RTD were obtained by injecting a tracer at the feeding section of the extruder and quantifying tracer concentration at the die exit. A red food colouring agent (E124) was used. One mL of a 2g.L^{-1} solution of this colouring agent was injected at t=0 at the feeding section with a syringe. Extrudate was collected in several samples, each one corresponding to a 10s time interval. Each sample was diluted in water and centrifuged at 10000g for 10 minutes (centrifuge KR22i Jouan S.A.S, Saint-Herblain, France). Supernatant tracer content was quantified by measuring absorbance at 507nm (UV–vis spectrophotometer UV2 Unicam, Cambridge, UK). It appeared that almost all tracer injected at the feeding section is recovered in the outgoing material supernatant during the experiments.

4.1.2. Simulation results

Few assumptions were adopted concerning some elements of the restrictive screw profile to perform simulations. Grooved reverse pitch elements and kneading elements were replaced by reverse screw elements (25mm long with a 16.6mm pitch and 50mm long with a 25mm pitch respectively). For each feed rates ratio, one of the two experimental RTD was used to adjust values of the parameter λ_1. Parameter λ_2 was defined in function of λ_1: $\frac{\lambda_2}{\lambda_1} = 10$, as axial dispersion is lower in the conveying zones than in the fully filled zones. This ratio value was adopted because it appeared as a good compromise between a too low value that would deteriorate the adjustment quality (minimization by the least squares method) and a too high value that would raise numerical problems during the resolution. Hence, for r=1, λ_1=100 m^{-1} and λ_2=1000 m^{-1} were used and for r=3, λ_1=160 m^{-1} and λ_2=1600 m^{-1}. In Figure 7, curves *a* and *b* correspond to parameters adjustment and curves *c* and *d* to simulations performed by means of the proposed model.

Simulation results presented in Figure 5 globally show that the proposed model provides good predictions of experimental RTD curves. Experimental data clearly highlight the influence of feed rates ratio on flow in the extruder. Increasing *r* (the flow rate being constant) leads to an increase of the mean residence time and a wider distribution for both screw profiles. Then, changing screw profile also induces flow modifications in the extruder. Screw profile 2 being more restrictive, the mean residence time increases and distribution is wider than for screw profile 1. The observed evolution was satisfactorily simulated by the proposed model.

4.2. Polymer extrusion

Data from literature have been used so as to validate the proposed model for another type of material. The work published by Puaux et al. (2000) has been chosen because all information needed to perform simulations were mentioned (screw profile, die design, material properties). RTD evolution was assessed for different screw speed values in the case of low density polyethylene extrusion with a BC21 type extruder (Clextral S.A.S., Fiminy, France). The material being different from the previous case, value of λ_1 parameter was modified. It was adjusted according to one of the four known experimental RTD curves: for N=150rpm, λ_1=150m^{-1}. Screw profile used by Puaux et al. (2000) is described in Figure 6 (profile 3). Figure 7 presents experimental data and predictions from the proposed model. Predictions were globally close to experimental RTD, with a correctly simulated shape. However, some imprecisions can be noticed. Distribution width was a little underestimated and predictions were a little time-lagged, particularly for high screw speed values. Despite these imprecisions, this second validation case confirms the ability of the proposed model to simulate and predict RTD curves from process and geometrical parameters even with the assumption of a constant viscosity along the screw.

5. CONCLUSION

In this paper, a new model is proposed to predict residence time distribution in fully intermeshing co-rotating twin-screw extruders, taking into account control parameters (screw speed and flow rate) and geometrical parameters (screw profile and die design). Possibilities offered by the proposed model were illustrated by simulations for various operating and geometrical conditions. Validation was performed for two different applications, seaweeds extrusion and polymer material extrusion. It showed the model ability to predict RTD for various kinds of extruded materials. The originality of the proposed model lies in its ability to predict RTD after adjusting only one parameter (λ_1) thanks to a unique experimental RTD curve. Once parameters adjustment is performed, RTD can be predicted for different operating conditions (screw speed and feed rate) and different geometrical configurations (screw profile and die design).

The proposed RTD model could be improved by adding several extensions. It could be extended to the reactive case by coupling reaction kinetics to the equation describing spatio temporal tracer concentration evolution (Equation 13). It would also be possible, provided other assumptions are made, to adapt the structure of equation 10 to take into account the case of an evolving viscosity along the screw channel. And if reaction advancement and viscosity are linked, it would also be possible to take it into account if the relation is correctly formalized. The coupling between kinetic model of alginate extraction and flow model will be discussed in a forthcoming paper. The extended model could be a useful tool to help optimizing reactive extrusion applications.

REFERENCES

Ainser, A., 1996. Etudes des écoulements et réactions chimiques en extrudeuse bi-vis. Approche expérimentale : utilisation de la distribution des temps de séjour. PhD thesis, Université de Saint-Etienne.

Baron, R., 1995. Modélisation et commande d'un procédé d'extrusion de pulpe de poisson. PhD thesis, Université Paris Sud.

Berzin, F., Hu, G.H., 2004. Procédés d'extrusion réactive. Techniques de l'Ingénieur, AM3654.

Carrot, C., Guillet, J., May, J.F., Puaux, J.P., 1993. Modeling of the conveying of solid polymer in the feeding zone of intermeshing co-rotating twin screw extruders. Polymer Engineering and Science, 33 (11), 700-708.

Dufaure, C., Mouloungui, Z., Rigal, L., 1999. A twin-screw extruder for oil extraction: II. Alcohol extraction of oleic sunflower seeds. Journal of the American Oil Chemists' Society, 76, 1081-1086.

Ganzeveld, K.J., Janssen, L.P.B.M., 1993. Twin screw extruders as polymerization reactors for free radical homo polymerization. The Canadian Journal of Chemical Engineering, 71, 411-418.

Janssen, L.P.B.M., Hollander, R.W., Spoor, M.W., Smith, J.M., 1979. Residence time distributions in a plasticating twin screw extruder. AIChE Journal, 25, 345-351.

N'Diaye, S., Rigal, L., Larocque, P., Vidal, P.F., 1996. Extraction of hemicelluloses from poplar, *Populus tremuloides*, using an extruder-type twin-screw reactor: a feasibility study. Bioresource Technology, 57, 61-67.

Pérez, R., Kaas, R., Campello, F., Arbault, S., Barbaroux, O., 1992. La culture des algues dans le monde. Ifremer, Plouzané, France.

Perrin, J.L., De Choudens, C., 1996. Extrusion technology in paper pulp processing. In: Proceedings of the Conference on '40 years of twin-screw extrusion at Clextral', Firminy, France, 8–10 October 1996.

Prat, L., Guiraud, P., Rigal, L., Gourdon, C., 1999. Two phase residence time distribution in a modified twin-screw extruder. Chemical Engineering and Processing, 38, 73-83.

Prat, L., Guiraud, P., Rigal, L., Gourdon, C., 2002. A one dimensional model for the prediction of extraction yields in a two phases modified twin-screw extruder. Chemical Engineering and Processing, 41, 743-751.

Puaux, J.P., Bozga, G., Ainser, A., 2000. Residence time distribution in a corotating twin-screw extruder. Chemical Engineering Science, 55, 1641-1651.

Puaux, J.P., Cassagnau, P., Bozga, G., Nagy, I., 2006. Modeling of polyurethane synthesis by reactive extrusion. Chemical Engineering and Processing, 45, 481-487.

Rouilly, A., Jorda, J., Rigal, L., 2006. Thermo_mechanical processing of sugar beet pulp. I. Twin-screw extrusion process. Carbohydrate Polymers, 66, 81-87.

Tadmor, A., Klein, I., 1970. Engineering Principles of Plasticating Extrusion. Van Nostrand Reinhold Company, New York.

Vauchel, P., Baron, R., Kaas, R., Arhaliass, A., Legrand, J., 2008a. A new process for extracting alginates from *Laminaria digitata* : reactive extrusion. Food and Bioprocess Technology : an International Journal, 1, 297-300.

Vauchel, P., Le Roux, K., Kaas, R., Arhaliass, A., Baron, R., Legrand, J., 2008b. Kinetics modeling of alginate alkaline extraction from *Laminaria digitata*. Bioresource Technology, 100,1291-1296.

Figure captions

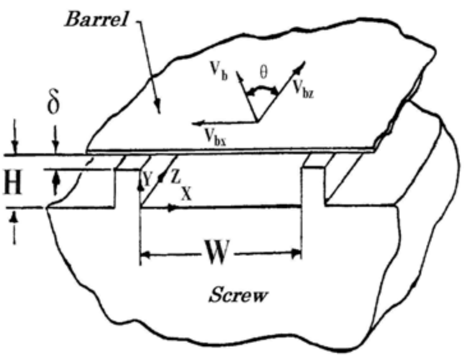

Figure 1. The unrolled channel and the moving plane barrel (Tadmor and Klein, 1970).

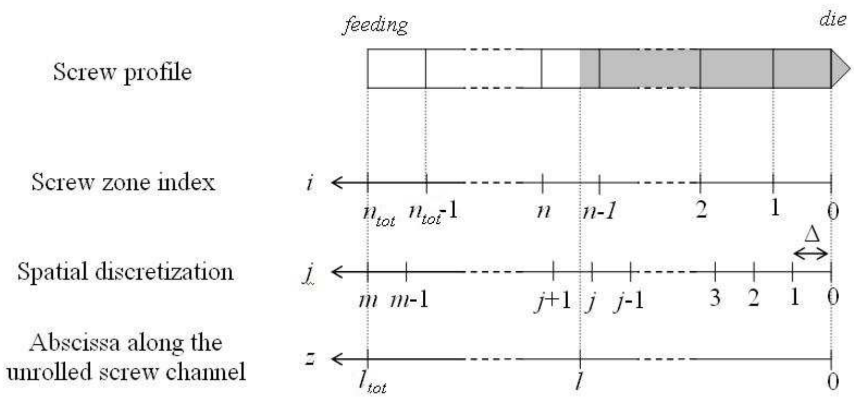

Figure 2. Screw profile, screw zone index, spatial discretization and abscissa along the unrolled screw channel.

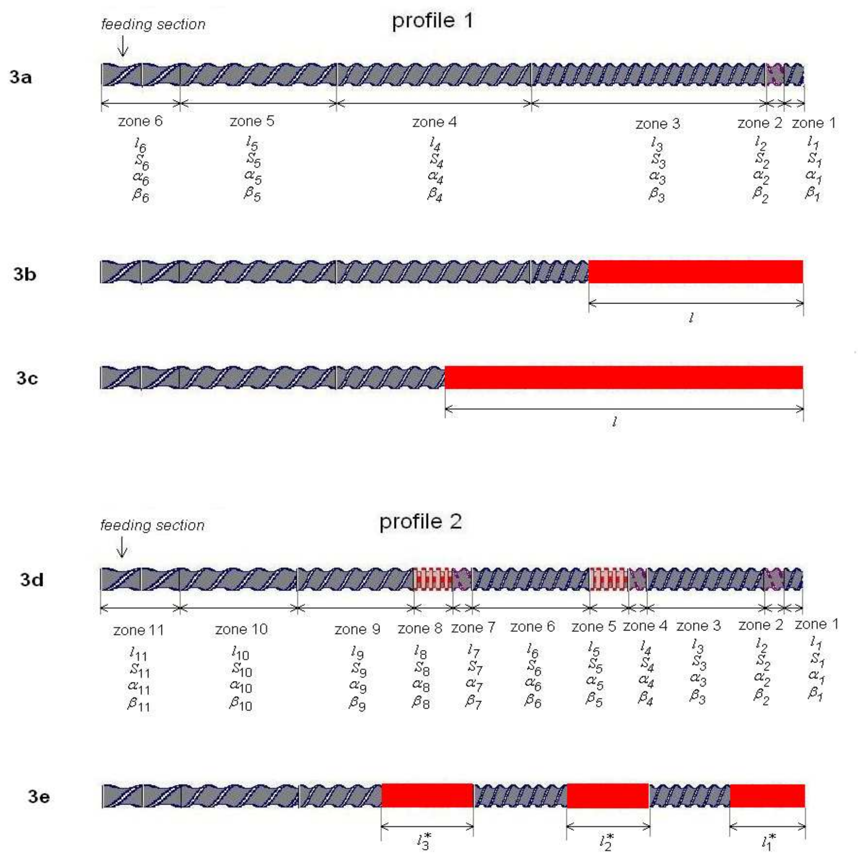

Figure 3. Screw profiles used for seaweeds extrusion experiments. (a) screw profile 1 and geometrical parameters associated; (b) case where $l<(l_3+l_2+l_1)$ with profile 1; (c) case where $(l_3+l_2+l_1)\leq l<(l_4+l_3+l_2+l_1)$ with profile 1; (d) screw profile 2 and geometrical parameters associated; (e) case of three different fully filled zones with profile 2 (and with $l_3^*<(l_9+l_8+l_7)$).

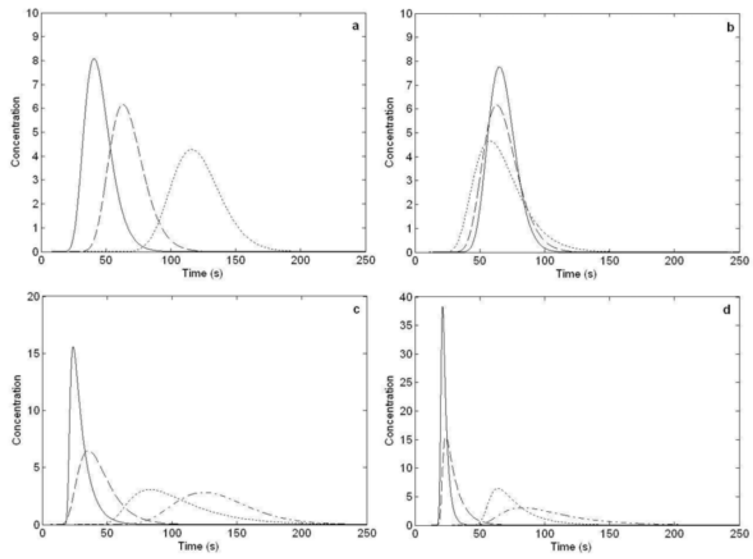

Figure 4. RTD simulations for different process and geometrical parameters. (a) different values of screw speed : (—) N=600rpm; (– –) N=400rpm; (---) N=200rpm (Q=5kg.h^{-1} ; p=50mm ; K=7.10^{-11}m^{3}). (b) different values of flow rate: (----) Q=3kg.h^{-1}; (– –) Q=5kg.h^{-1}; (—) Q=7kg.h^{-1} (N=400rpm ; p=50mm ; K=7.10^{-11}m^{3}). (c) different values of screw pitch and screw speed : (---) N=200rpm and p=25mm ; (– - –) N=200rpm and p=50mm ; (—) N=600rpm and p=25mm ; (– –) N=600rpm and p=50mm (Q=5kg.h^{-1} ; K=7.10^{-11}m^{3}). (d) different values of die restriction coefficient and screw speed : (—) N=600rpm and K=1,5.10^{-10}m^{3} ; (– –) N=600rpm and K=7.10^{-11}m^{3}; (----) N=200rpm and K=1,5.10^{-10}m^{3}; (– - –) N=200rpm and K=7.10^{-11}m^{3} (Q=5kg.h^{-1} ; p=25mm).

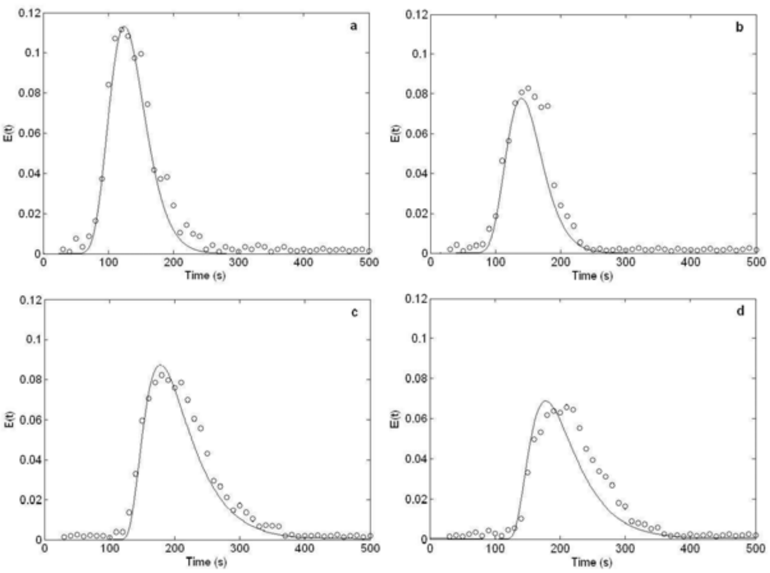

Figure 5. Model validation for seaweeds extrusion for two different screw profiles and feed rates ratios. (O) experimental data; (—) model prediction. Parameters adjustment : (a) screw profile 1 and r=1; (b) screw profile 1 and r=3. Simulations: (c) screw profile 2 and r=1; (d) screw profile 2 and r=3.

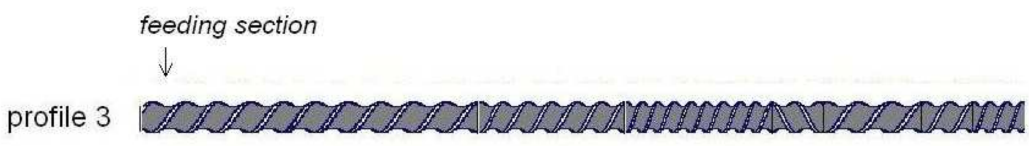

Figure 6. Screw profile 3 used by Puaux et al. (2000) for LDPE extrusion.

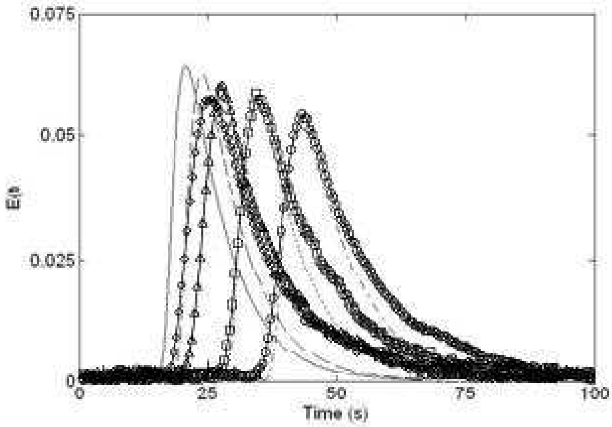

Figure 7. Model validation for polymer extrusion. Experimental data: (◊) *N*=400rpm; (Δ) *N*=300rpm; ( ) *N*=200rpm; (O) *N*=150rpm. Model prediction: (—) *N*=400rpm; (– –) *N*=300rpm; (----) *N*=200rpm; (– - –) *N*=150rpm.